Numerical investigation on the supersonic flow around a saboted bullet

Quang Tuan Nguyen[a], *Hai Minh* Nguyen[b], *Xuan Son* Bui[c]

Le Quy Don Technical University, Faculty of Special Equipment, Hanoi, Socialist Republic of Vietnam

[a] e-mail: tuanmoscow2004@gmail.com, **corresponding author**, ORCID iD: https://orcid.org/0000-0002-7741-8232

[b] e-mail: nguyenhaiminhtb2013@gmail.com, ORCID iD: https://orcid.org/0000-0002-5170-6228

[c] e-mail: buixuanson.mta@gmail.com, ORCID iD: https://orcid.org/0000-0003-4520-5168

https://doi.org/10.5937/vojtehg72-48837

FIELD: mechanical engineering, fluid dynamics
ARTICLE TYPE: original scientific paper

Abstract:

Introduction/purpose: In this paper, the aerodynamic characteristics of a special bullet were investigated at supersonic conditions. A model of a handgun saboted bullet was selected for the study.

Methods: The method used in the research was computational fluid dynamic (CFD) simulation. The turbulence model k-ε was used for numerical calculation. The air model was selected as an ideal gas. For air viscosity, the Sutherland model was applied.

Results: The numerical simulation results show the behavior of the supersonic flow over the saboted bullet. By varying the petals opening angle and bullet velocity, their influences on the drags of the sabot and the penetrator were obtained to be used for later sabot separation study.

Conclusion: The study shows that the CFD simulation approach can be implemented to analyze the aerodynamic drags on the sabot and the penetrator after the saboted bullet leaving the gun barrel. The simulation results obtained in this work are important in designing saboted light armor-piercing bullets fired from handguns.

Key words: saboted bullets, handgun, aerodynamic characteristics, Ansys Fluent, CFD, numerical simulation.

Introduction

Increasing the performances of weapon systems is always necessary for any army in the world. Modern ballistic vests are effective against standard bullets (Odanović & Bobić, 2003; Stopforth & Adali, 2019; Yaneva, 2020; Zochowski et al, 2021). This fact prompts weapon

designers to find new ways to enhance the penetrating ability of bullets. One method is to use saboted bullets. This kind of bullets consists of a light-weight polymer sabot, an aluminum supporting base and a penetrator made of heavy-weight material (depleted uranium, tungsten carbide, etc.). After exiting the gun muzzle, the penetrator separates from the sabot and continues flying to the target alone. Due to high muzzle velocity and a small cross-sectional area, the penetrator delivers a very high penetrating performance (Abdelsalam & Fayed, 2022). Such a bullet structure has been successfully implemented in some weapon systems such as American 7.62x51mm M948 and 12.7x99mm M903 (Starek & Stepniak, 2021), 6.5x25mm CBJ (CBJ Tech, 2024) and Singaporean 12.7mm SLAP (Ministry of Defence, Singapore, 2016). Compared to standard bullets, saboted bullets own significant advantages: better penetrating performance; higher hit probability; longer range; higher impact velocity; lower levels of barrel wear and corrosion; and non-toxicity since they do not contain lead. They are effective against all targets of small arms, such as light ground vehicles, helicopters, etc. as well as highly protected troops. Their typical structure is presented in Figure 1.

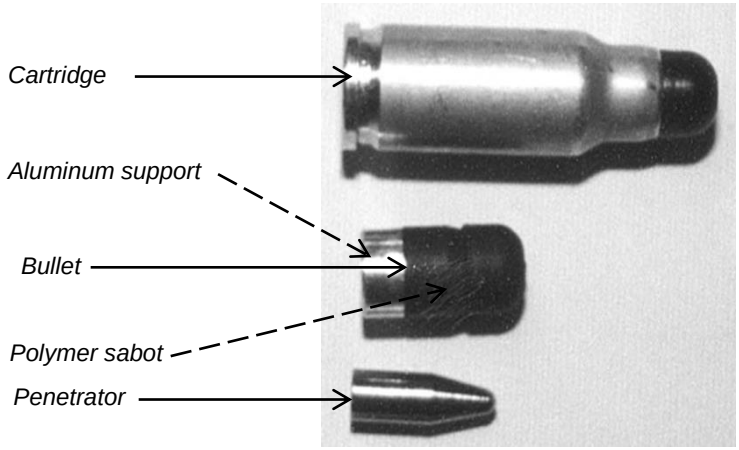

Figure 1 – Structure of the 6.5x25mm CBJ cartridge and the bullet

The working principle of the saboted bullet is as follows: after exiting the gun muzzle, under high centrifugal and aerodynamic forces, the sabot undergoes deformation when the sabot petals open at some angle increasing the sabot area exposed to air flow. Consequently, the drag on the sabot is much greater than the drag on the penetrator. Due to this drag difference, the penetrator gradually separates from the sabot. The sabot separation process is illustrated in Figure 2. After separating from the

penetrator, the sabot remains intact and continues on its intended course. Eventually, the sabot descends to the ground.

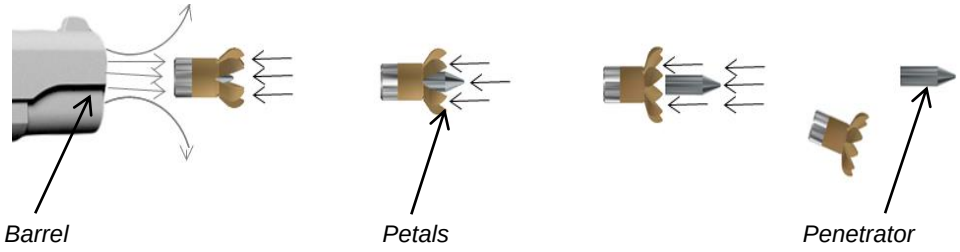

Figure 2 – Sabot separation process

In the saboted bullet designing process, one of the crucial problems is to investigate the interaction between the air and the bullet under different conditions. Although there is a significant number of studies on the separation process of the armour-piercing fin-stabilized discarding sabot (Lin & Lai, 1997; Huang et al, 2014; Lesage & Girard, 1996; Patanwala et al, 2023), the separation process of saboted bullets has not been appropriately studied. The present work aims at studying the aerodynamic characteristics of the supersonic flow around a saboted bullet, including the drags acting on the sabot and the penetrator at various muzzle velocities and petals opening angles. The muzzle velocity ranges from 500m/s to 600m/s with an increment of 20m/s. The petals opening angle changes in the interval from 50^0 to 80^0 with an increment of 10^0. The remaining structural parameters of the bullet are unchanged according to ballistic restrictions and designing requirements.

Numerical approach

Geometry model

In this research, a saboted bullet intended to be fired from 7.62mm caliber handguns has been considered for investigation. The bullet geometry details are presented in Figure 3. All the dimensions are presented in mm. The bullet consists of three components: a penetrator, a sabot with 6 petals, and an aluminium support as in the case of the 6.5x25mm CBJ structure.

The investigated air domain is shown in Figure 4. The domain length, width and height are 40L, 10L and 10L, respectively. Here, L is the overall length of the saboted bullet (L = 17.5mm in our case). The air domain was

created big enough to properly describe the turbulent flow behind the sabot.

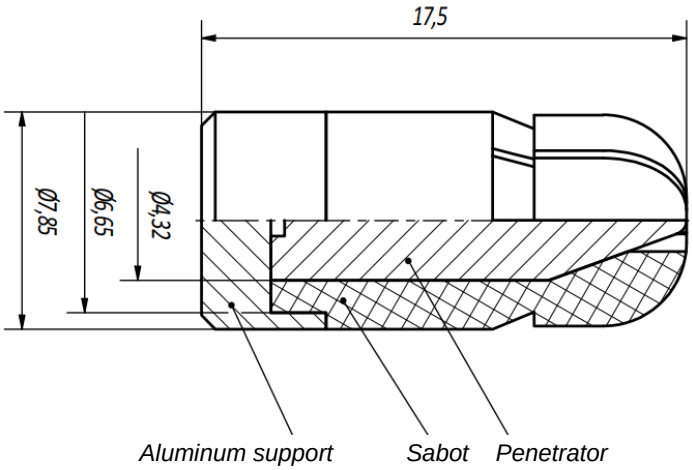

Figure 3 – Bullet dimensions (in mm)

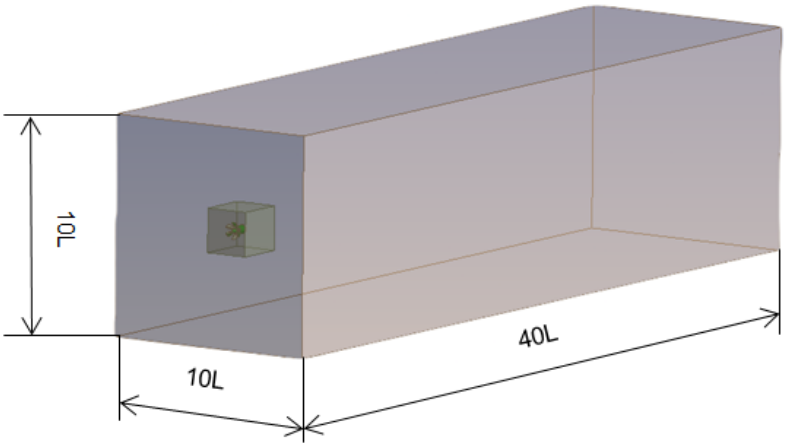

Figure 4 – Air domain dimensions

Mesh generation

In order to reduce burden on the mesh generation procudure, the aluminum support and the sabot were modeled as a unified object. This simplification does not affect the simulation accuracy since the aluminum support and the sabot are securely connected with each other and stay together for the whole separation process. Based on the bullet structure

and accuracy, the computational domain grid around the bullet was automatically generated. Figure 5 shows the mesh generation results on the bullet surface. There are a total of 3 365 498 mesh elements.

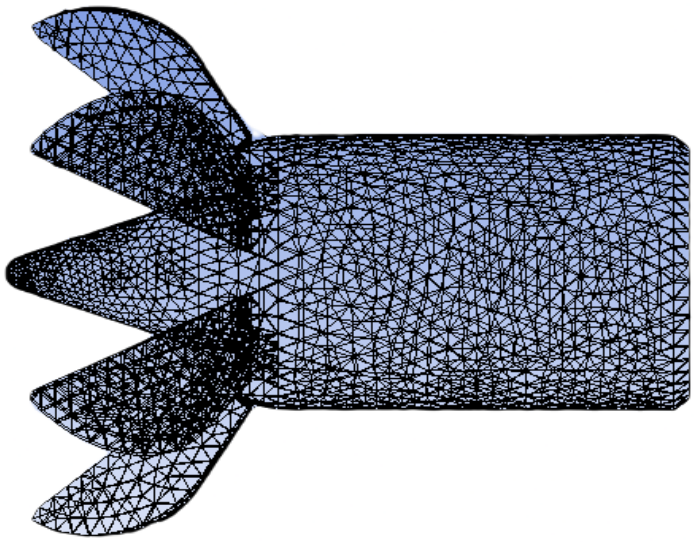

Figure 5 – Mesh around the bullet

Mathematical model

In this research, the Reynolds averaged Navier-Stokes (RANS) equations were selected to calculate the drag and analyze the flow fields around the bullet model. In the RANS methods, an averaged filter was applied to the Navier-Stokes equations. The Reynolds stresses are simulated by turbulent models. Despite only supporting averaged flow fields, the RANS approach is greatly effective at saving calculation time while maintaining a high level of accuracy. There are five Navier-Stokes equations: the first one expresses the law of conservation of mass, the next three describe the law of conservation of momentum, and the last one represents the law of conservation of energy (Matsson, 2023). They are as follows:

$$\frac{\partial p}{\partial t}+\frac{\partial(\rho u)}{\partial x}+\frac{\partial(\rho v)}{\partial y}+\frac{\partial(\rho w)}{\partial z}=0, \tag{1}$$

$$\frac{\partial(\rho u)}{\partial t}+\frac{\partial(\rho u^2)}{\partial x}+\frac{\partial(\rho uv)}{\partial y}+\frac{\partial(\rho uw)}{\partial z}= \\ =-\frac{\partial p}{\partial x}+\frac{1}{Re}(\frac{\partial(\tau_{xx})}{\partial x}+\frac{\partial(\tau_{xy})}{\partial y}+\frac{\partial(\tau_{xz})}{\partial z}), \quad (2)$$

$$\frac{\partial(\rho v)}{\partial t}+\frac{\partial(\rho uv)}{\partial x}+\frac{\partial(\rho v^2)}{\partial y}+\frac{\partial(\rho vw)}{\partial z}= \\ =-\frac{\partial p}{\partial y}+\frac{1}{Re}(\frac{\partial(\tau_{xy})}{\partial x}+\frac{\partial(\tau_{yy})}{\partial y}+\frac{\partial(\tau_{yz})}{\partial z}), \quad (3)$$

$$\frac{\partial(\rho w)}{\partial t}+\frac{\partial(\rho uw)}{\partial x}+\frac{\partial(\rho vw)}{\partial y}+\frac{\partial(\rho w^2)}{\partial z}= \\ =-\frac{\partial p}{\partial z}+\frac{1}{Re}(\frac{\partial(\tau_{xz})}{\partial x}+\frac{\partial(\tau_{yz})}{\partial y}+\frac{\partial(\tau_{zz})}{\partial z}), \quad (4)$$

$$\frac{\partial(E_T)}{\partial t}+\frac{\partial(uE_T)}{\partial x}+\frac{\partial(vE_T)}{\partial y}+\frac{\partial(wE_T)}{\partial z}= \\ =-\frac{\partial(up)}{\partial x}-\frac{\partial(vp)}{\partial y}-\frac{\partial(wp)}{\partial z}+ \\ +\frac{1}{Re}\left[\frac{\partial}{\partial x}\left(u\tau_{xx}+v\tau_{xy}+w\tau_{xz}\right)+\frac{\partial}{\partial y}\left(u\tau_{xy}+v\tau_{yy}+w\tau_{yz}\right)+\right. \\ \left.+\frac{\partial}{\partial z}\left(u\tau_{xz}+v\tau_{yz}+w\tau_{zz}\right)\right]-\frac{1}{Re}\frac{1}{Pr}\left(\left[\frac{\partial q_x}{\partial x}+\frac{\partial q_y}{\partial y}+\frac{\partial q_z}{\partial z}\right), \quad (5)$$

where u, v and w respectively are the velocity in the x, y and z directions; p is the pressure, t is the time, ρ is the air density, τ is the deviatoric stress tensor, E_T is the total energy, q is the heat flux, Re is the Reynolds number, and Pr is the Prandtl number.

In order to analyze the high-speed compressible flow around a saboted bullet, the k-ε turbulence model was applied. Introduced in 1974 (Launder & Spalding, 1974), this model quickly became one of the most popular models used in computational fluid dynamics to analyze aerodynamic characteristics for turbulent flow conditions. It is suitable for

high Reynolds numbers or free stream flow. Various authors have been successfully implementing the *k-ε* turbulence model to predict aerodynamic characteristics and analyze the flow around bodies with complicated geometry involving separation and strong pressure fluctuation (Do et al, 2022; Dolzhikov & Nikolaev, 2015; Ko et al, 2020; Trakic, 2020). The *k-ε* turbulence model enables turbulent eddy viscosity to be taken into account using the kinetic energy *k* and the dissipation rate *ε*. These additional parameters are determined through the following equations:

$$\frac{\partial(\rho k)}{\partial t}+u\frac{\partial(\rho k)}{\partial x}+v\frac{\partial(\rho k)}{\partial y}+w\frac{\partial(\rho k)}{\partial z}=\frac{\partial}{\partial x}\left[\left(\mu+\frac{\mu_t}{\sigma_k}\right)\frac{\partial k}{\partial x}\right]+ \\ =\frac{\partial}{\partial y}\left[\left(\mu+\frac{\mu_t}{\sigma_k}\right)\frac{\partial k}{\partial y}\right]+\frac{\partial}{\partial z}\left[\left(\mu+\frac{\mu_t}{\sigma_k}\right)\frac{\partial k}{\partial z}\right]+P_k-\rho\varepsilon, \tag{6}$$

$$\frac{\partial(\rho\varepsilon)}{\partial t}+u\frac{\partial(\rho\varepsilon)}{\partial x}+v\frac{\partial(\rho\varepsilon)}{\partial y}+w\frac{\partial(\rho\varepsilon)}{\partial z}=\frac{\partial}{\partial x}\left[\left(\mu+\frac{\mu_t}{\sigma_k}\right)\frac{\partial \varepsilon}{\partial x}\right]+ \\ =\frac{\partial}{\partial y}\left[\left(\mu+\frac{\mu_t}{\sigma_k}\right)\frac{\partial \varepsilon}{\partial y}\right]+\frac{\partial}{\partial z}\left[\left(\mu+\frac{\mu_t}{\sigma_k}\right)\frac{\partial \varepsilon}{\partial z}\right]+P_k C_{1\varepsilon}\frac{\varepsilon}{k}-\rho C_{2\varepsilon}\frac{\varepsilon^2}{k}, \tag{7}$$

where the function P_k is defined as:

$$P_k=\tau_{xx}\frac{\partial u}{\partial x}+\tau_{xy}\frac{\partial u}{\partial y}+\tau_{xz}\frac{\partial u}{\partial z}+\tau_{yx}\frac{\partial v}{\partial x}+\tau_{yy}\frac{\partial v}{\partial y}+\tau_{yz}\frac{\partial v}{\partial z}+ \\ +\tau_{zx}\frac{\partial w}{\partial x}+\tau_{zy}\frac{\partial w}{\partial y}+\tau_{zz}\frac{\partial w}{\partial z}, \tag{8}$$

where *k* is the kinetic energy, *ε* is the dissipation rate, E_{ij} represents the component of the rate of deformation, and μ_t represents the eddy viscosity. *C1ε, C2ε,* σ_k and σ_ε are constant numbers: $C_{1\varepsilon}$ = 1.44, $C_{2\varepsilon}$ = 1.92, σ_k =1.00 and σ_ε = 1.30.

The turbulent viscosity μ_t is calculated using the equation below:

$$\mu_t=\rho C_\mu\frac{k^2}{\varepsilon}, \tag{9}$$

where the parameter C_μ is a constant number, C_μ = 0.0845.

Boundary condition and convergence criteria

The abovementioned Navier-Stokes equations from (1) to (9) were solved using Ansys Fluent numerical simulation software. The RANS equations with the k-ε turbulent model were applied in this research. The density-based solver was used. The finite volume method with the second order of numerical accuracy for pressure, density, momentum, and turbulent kinetic energy was employed for the investigation. The air model was an ideal gas. The Coupled algorithm was implemented for the calculation. The calculation domain was defined with the following boundary conditions: inlet, outlet, and wall. Velocity, static pressure, and static temperature were established for the inlet flow. For the outlet flow, static pressure was defined. Other setup parameters are presented in Table 1.

Table 1 – Ansys Fluent simulation settings

Parameter	**Value**
Inlet velocity	Bullet's muzzle velocity
Gauge pressure	0 Pascal
Side	Symmetry
Wall	No slip wall
Viscosity model	Sutherland
Temperature	300 K
Convergence criteria	10^{-6}

Validation

Although the numerical method and the simulation procedure have been carefully selected and carried out in this study, the obtained results should be compared with experimental data to verify the accuracy of the results. Since no relevant experimental data has been published in open literature so far, some limitations do exist regarding the result validation. However, the main objective of this research is to investigate the effect of the muzzle velocity of a bullet and the angle of petals opening on the drag trend of the sabot and the penetrator; hence, experimental tests can be conducted later as part of the continuation of this work to validate and verify the overall calculation model for the separation phenomenon.

Results and discussion

Flow field around the bullet

The pressure distribution around the bullet on the symmetric plane is presented in Figure 6. Obviously, the pressure is the highest in the forepart of the bullet while the pressure is significantly lower in the aftpart in comparison with that in the forepart. Figure 7 shows the velocity field around the bullet at a bullet velocity of 600 m/s and an angle of petals opening of 80^0. The flow separation takes place on the rear surface of the sabot petals. The turbulence intensity of the flow is presented in Figure 8. The most intense turbulence occurs in the space behind the opening petals.

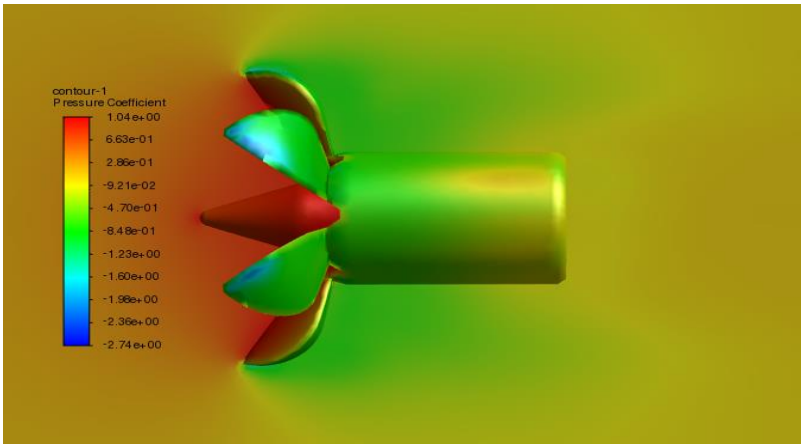

Figure 6 – Pressure distribution around the bullet (petals opening angle: 80^0, bullet velocity: 600 m/s)

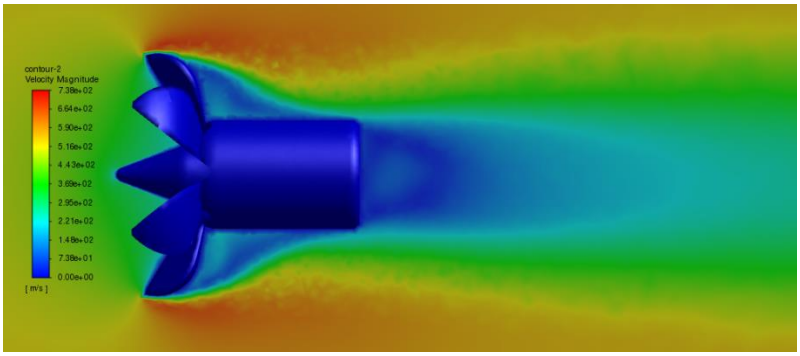

Figure 7 – Velocity distribution around the bullet (petals opening angle: 80^0, bullet velocity: 600 m/s)

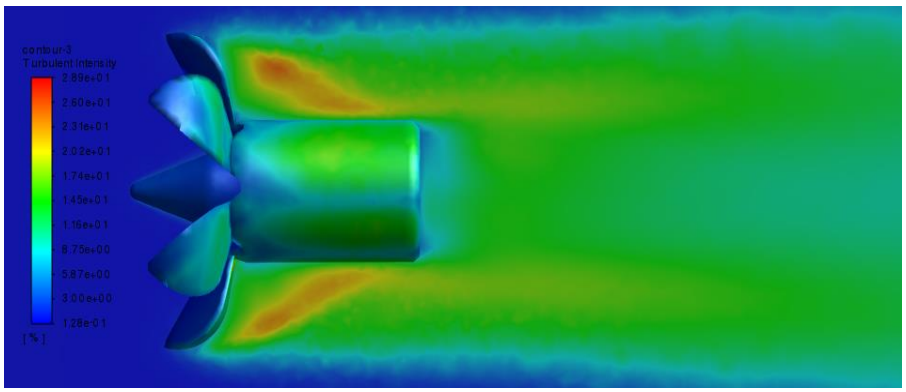

Figure 8 – Turbulence intensity around the bullet (petals opening angle: 80^0, bullet velocity: 600 m/s)

Influence of bullet velocity on drag

Since bullet velocity is a defining parameter for exterior ballistic fundamental problem solving, it is important to determine the drag of the sabot and the penetrator for different velocities.

Moreover, the muzzle velocity of the bullet is one of the defining parameters for the fundamental interior ballistic problem. In the penetrator-sabot separation process, the bullet velocity gradually changes and, as a consequence, the air drag acting on the sabot and the penetrator will change. In this study, the drag of the sabot and the drag of the penetrator were obtained for the velocity values ranging from 500 m/s to 600 m/s with different petals opening angles.

The influence of velocity on the drag of the sabot and the drag of the penetrator are shown in Figure 9, Figure 10, and Figure 11. Clearly, for all values of petals opening angles, an evident tendency can be seen: the greater bullet velocity, the greater the drags of the sabot and the penetrator; the greater bullet velocity, the greater difference of the drags on the sabot and the penetrator.

This means that the sabot and the penetrator leave each other quicker with a higher bullet velocity. Additionally, the drag-velocity dependency is almost linear for all the values of petals opening angles.

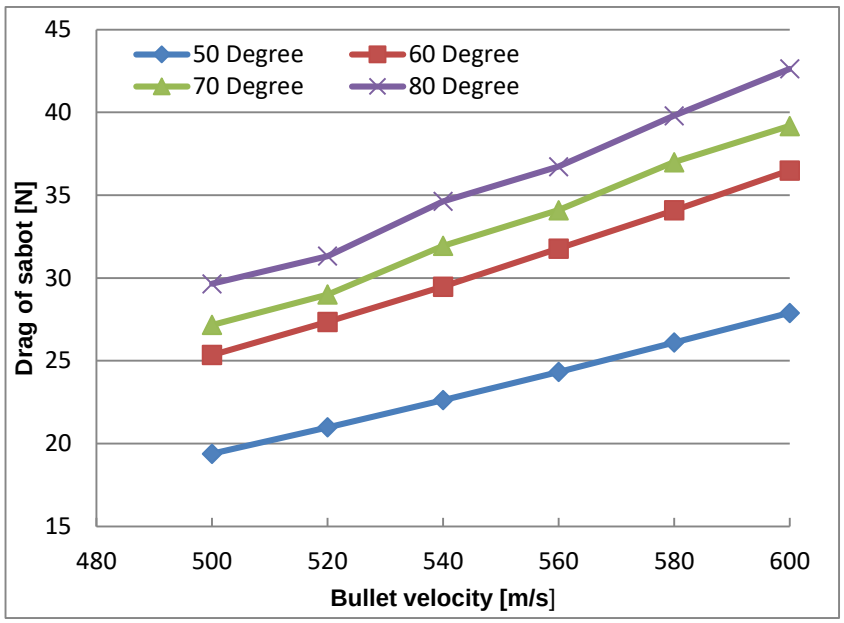

Figure 9 – Influence of bullet velocity on sabot drag for various petals opening angles

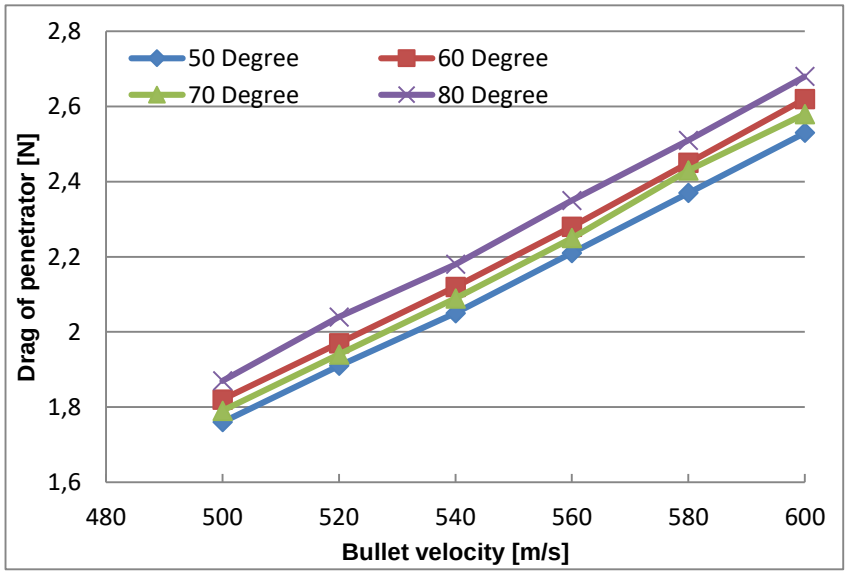

Figure 10 – Influence of bullet velocity on penetrator drag for various petals opening angles

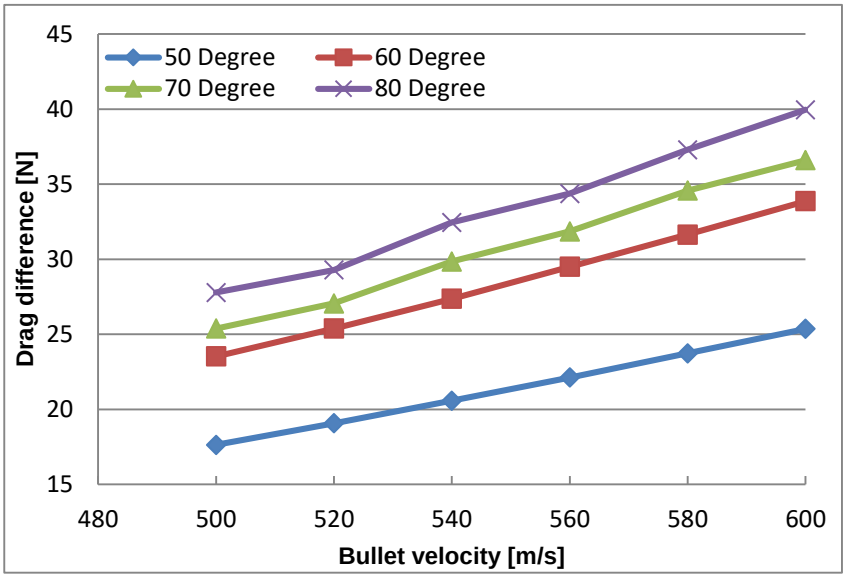

Figure 11 – Influence of bullet velocity on the difference of the drags of the sabot and the penetrator for various petals opening angles

Influence of petals opening angles on drag

In the sabot separation process, the petals opening angle graduallly changes affecting the air flow state around the bullet and the aerodynamic interference between the sabot and the penetrator. Consequently, the drag of the sabot and the drag of the penetrator change with time. Therefore, it is of great interest to investigate how the drag of the sabot and the drag of the penetrator change with the changes of petals opening angles. In this study, the petals opening angle varies from 50^0 to 80^0 with an increment of 10^0. Figure 12 - Figure 14 show the effect of petals opening angles on the drag of the sabot, the drag of the penetrator and their difference for various bullet velocities. Obvious tendencies can be observed. For any value of bullet velocity, the drag of the sabot, the difference between the drag of the sabot and the drag of the penetrator increase quickly with the increase of the angle of petals opening. Consequently, the greater the petals opening angle, the more quickly the sabot and the penetrator leave each other. Hence, one can vary the material or/and the structural parameters of the sabot, e.g. the sabot length, to influence the penetrator-sabot separation process.

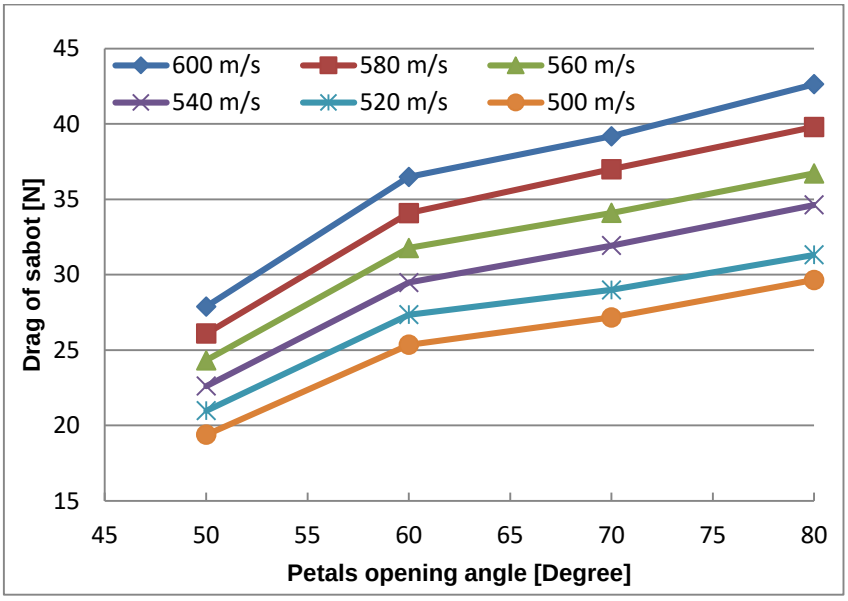

Figure 12 – Influence of the petals opening angle on the drag of the sabot for various bullet velocities

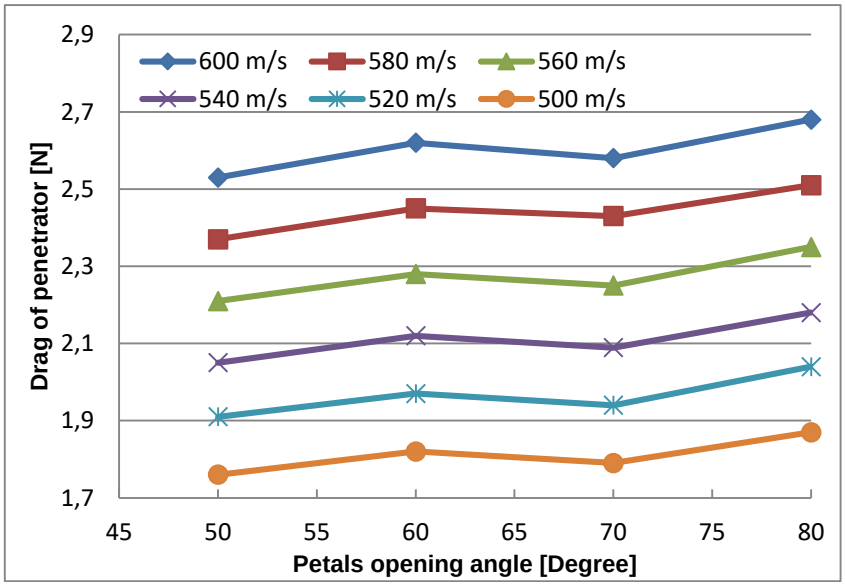

Figure 13 – Influence of the petals opening angle on the drag of the penetrator for various bullet velocities

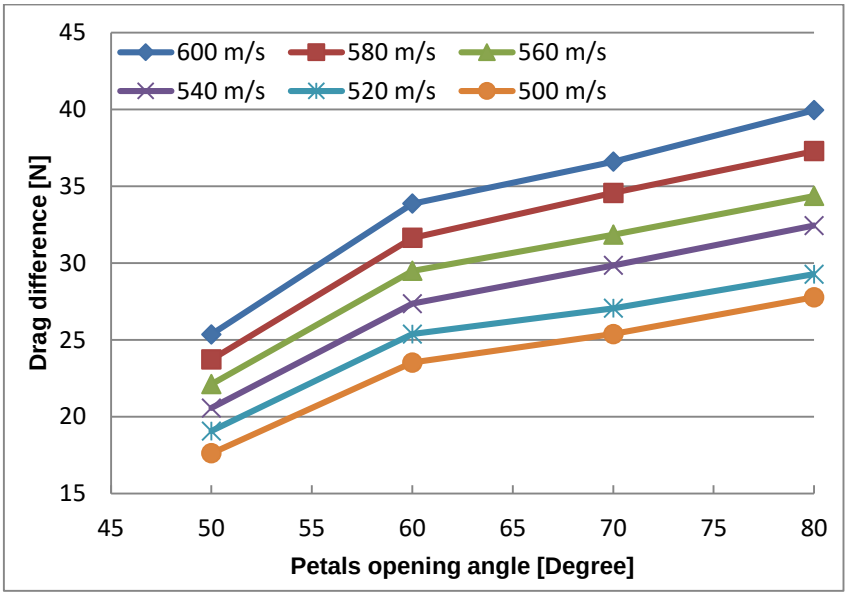

Figure 14 – Influence of the petals opening angle on the difference of the drags of the sabot and the penetrator for various bullet velocities

Conclusion

In this research, in order to save experimental time and resources, the numerical method was used to investagate the flow around a sub-caliber saboted bullet and analyze the effect of bullet velocity and the sabot petals opening angle on the drags of the sabot and the penetrator. The following are the main conclusions derived from the study:

The numerical method is a powerful and effective tool to study the air flow phenomenon around a complex body such as a saboted bullet, especially to predict the drags of the sabot and the penetrator under different conditions.

The pressure distribution around the bullet is complex: the pressure is the highest in the forepart and significantly lower in the aftpart.

The most intense turbulence takes place in the space behind the opening petals. The drag of the sabot, the drag of penetrator and their difference are almost linearly dependant on bullet velocity for any certain petals opening angle.

With increasing the petals opening angle, the drag of the sabot and the difference of the drag of the sabot and drag of the penetrator increase very quickly.

The overall tendency is that the greater bullet velocity or the petals opening angle are, the more quickly the penetrator leaves the sabot.

Eventually, the results obtained in this research work can be applied for further study and development of sub-calibre saboted bullets with similar geometries.

Future work

The following directions are recommended for further continuation of this study:

The first direction is to determine the drags of the sabot and the penetrator depending on their relative movement while the penetrator gradually leaves the sabot.

The second direction is to implement approximation techniques to present the drags of the sabot and the penetrator in form of continuous functions of velocity, opening angle and relative movement for further usage in sabot separation studies.

The third direction is to use continous functions of drags of the sabot and the penetrator in solving the fundamental exterior ballistic problem of a saboted bullet to determine not only the penetrator velocity at the moment it leaves the sabot but also the distance from the gun muzzle to the separation point and then to conduct experimental tests to verify the comprehensive calculation model.

References

Abdelsalam, O.R. & Fayed, A. 2022. Tungsten carbide core 12.7x99mm AP projectiles ballistic behavior against high hardness steel armor. *Journal of Physics: Conference Series,* 2299, art.number:012017. Available at: https://doi.org/10.1088/1742-6596/2299/1/012017.

-CBJ Tech. 2024. *6.5x25 CBJ APDS Tungsten core inside a discarding sabot. Cbjtech.com* [online]. Available at: https://www.cbjtech.com/ammunition/6-5x25-cbj/6-5x25-cbj-apds/ [Accessed: 21 December 2023].

Do, V.M., Tran, T.H., Bui, X.S. & Le, D.A. 2022. Influence of spike-nosed length on aerodynamic drag of a wing-projectile model. *Advances in Military Technology*, 17(1), pp.33-45. Available at: https://doi.org/10.3849/aimt.01542.

Dolzhikov, V.I. & Nikolaev, A.V. 2015. Determination of aerodynamic characteristics of rotating aircraft in the uncontrolled flight by means of engineering analysis systems. *Aerospace MAI Journal*, 22(3), pp.47-53 [online]. Available at: https://vestnikmai.ru/eng/publications.php?ID=58907&eng=Y (in Russian) [Accessed: 20 January 2024].

Huang, Z.-g., Wessam, M.E. & Chen, Z.-h. 2014. Numerical investigation of the three-dimensional dynamic process of sabot discard. *Journal of Mechanical Science and Technology*, 28, pp.2637-2649. Available at: https://doi.org/10.1007/s12206-014-0620-6.

Ko, A., Chang, K., Sheen, D.-J., Lee, C.-H., Park, Y. & Park, S.W. 2020. Prediction and Analysis of the Aerodynamic Characteristics of a Spinning Projectile Based on Computational Fluid Dynamics. *International Journal of Aerospace Engineering*, 2020, art.ID:6043721. Available at: https://doi.org/10.1155/2020/6043721.

Launder, B.E. & Spalding, D.B. 1974. The numerical computation of turbulent flows. *Computer Methods in Applied Mechanics and Engineering*, 3(2), pp.269-289. Available at: https://doi.org/10.1016/0045-7825(74)90029-2.

Lesage, F. & Girard, B. 1996. Wind tunnel and CFD investigation of aerodynamic interactions during sabot separation. In: *34th Aerospace Sciences Meeting and Exhibit*, Reno, NV, USA, January 15-18. Available at: https://doi.org/10.2514/6.1996-193.

Lin, H. & Lai, C.-L. 1997. Systematic study and numerical simulation of sabot projectile aerodynamics. *Journal of the Chinese Institute of Engineers*, 20(3), pp.275-284. Available at: https://doi.org/10.1080/02533839.1997.9741831.

Matsson, J.E. 2023. *An Introduction to Ansys Fluent 2023*. Mission, KS, USA: SDC Publications. ISBN: 978-1-63057-648-6.

-Ministry of Defence, Singapore. 2016. *Engineering land systems*. Singapore: Ministry of Defence [online]. Available at: https://www.mindef.gov.sg/oms/dam/publications/eBooks/DTC50/Engineering-Land-Systems.pdf [Accessed: 20 January 2024]. ISBN: 978-981-11-1490-8.

Odanović, Z. & Bobić, B. 2003. Ballistic protection efficiency of composite ceramics/metal armours. *Scientific Technical Review*, 53(3), pp.30-38 [online]. Available at: http://www.vti.mod.gov.rs/ntp/rad2003/3-03/odan/odan.pdf [Accessed: 20 January 2024].

Patanwala, H., Suresh, C. & Pawar, V. 2023. Computational Study of Safe Separation of Sabot from Penetrator in APFSDS. In: Edwin Geo, V. & Aloui, F. (Eds.) *Energy and Exergy for Sustainable and Clean Environment*, Volume 2, Green Energy and Technology, pp.279-294. Singapore: Springer. Available at: https://doi.org/10.1007/978-981-16-8274-2_19.

Starek, W. & Stepniak, W. 2021. Analysis and evaluation of small arms and ammunition with the reference to known foreign developments. *Problemy Techniki Uzbrojenia/Issues of Armament Technology,* R.35, z.99 pp.65-89. Available at: https://yadda.icm.edu.pl/baztech/element/bwmeta1.element.baztech-article-PWAA-0025-0007 (in Polish) [Accessed: 20 January 2024].

Stopforth, R. & Adali, S. 2019. Experimental study of bullet-proofing capabilities of Kevlar, of different weights and number of layers, with 9 mm projectiles. *Defence Technology*, 15(2), pp.186-192. Available at: https://doi.org/10.1016/j.dt.2018.08.006.

Trakic, A. 2020. Axial force coefficient of APFSDS projectile. *Defense and Security Studies*, 1(1), pp.1-15. Available at: https://doi.org/10.37868/dss.v1.id63.

Yaneva, S. 2020. Ballistic resistance of bulletproof vests level IIIA. Development of testing methodology. *MATEC Web of Conferences,* 317, art.number:06003. Available at: https://doi.org/10.1051/matecconf/202031706003.

Zochowski, P., Bajkowski, M., Grygoruk, R., Magier, M., Burian, W., Pyka, D., Bocian, M. & Jamroziak, K. 2021. Ballistic Impact Resistance of Bulletproof Vest Inserts Containing Printed Titanium Structures. *Metals,*11(2), art.number:225. Available at: https://doi.org/10.3390/met11020225.

Investigación numérica sobre el flujo supersónico alrededor de una bala saboteada

Quang Tuan Nguyen*,* **autor de correspondencia**,
Hai Minh Nguyen*, Xuan Son* Bui

Universidad Técnica Le Quy Don, Facultad de Equipos Especiales,
Hanói, República Socialista de Vietnam

CAMPO: mecánica, dinámica de fluidos
TIPO DE ARTÍCULO: artículo científico original

Resumen:

Introducción/objetivo: En este artículo, se investigaron las características aerodinámicas de una bala especial en condiciones supersónicas. Para el estudio se seleccionó un modelo de bala saboteada por pistola.

Métodos: El método utilizado en la investigación fue la simulación de dinámica de fluidos computacional (CFD). Para el cálculo numérico se utilizó el modelo de turbulencia k-ε. Se seleccionó el modelo aire como gas ideal. Para la viscosidad del aire se aplicó el modelo de Sutherland.

Resultados: Los resultados de la simulación numérica muestran el comportamiento del flujo supersónico sobre la bala saboteada. Al variar el ángulo de apertura de los pétalos y la velocidad de la bala, se obtuvo su influencia en las resistencias del casquillo y del penetrador para su posterior estudio de separación del casquillo.

Conclusión: El estudio muestra que el enfoque de simulación CFD se puede implementar para analizar las resistencias aerodinámicas en el casquillo y el penetrador después de que la bala saboteada sale del cañón del arma. Los resultados de la simulación obtenidos en este trabajo son importantes en el diseño de balas perforantes ligeras saboteadas disparadas con pistolas.

Palabras claves: balas saboteadas, pistola, características aerodinámicas, Ansys Fluent, CFD, simulación numérica.

Численное исследование сверхзвукового обтекания подкалиберной пули с отделяющимся поддоном

Куанг Туан Нгуен, **корреспондент,** *Хай Минь* Нгуен, *Сюань Сон* Буй

Государственный технический университет им. Ле Куй Дона,
факультет «Специальное машиностроение»,
г. Ханой, Социалистическая Республика Вьетнам

РУБРИКА ГРНТИ: 30.17.33 Газовая динамика,
30.17.53 Прикладная аэродинамика
ВИД СТАТЬИ: оригинальная научная статья

Резюме:

Введение/цель: В данной статье исследованы аэродинамические характеристики гиперзвукового патрона. Для исследования была выбрана модель пистолетного патрона с отделяющимся поддоном.

Методы: В исследовании использовался метод компьютерного моделирования гидродинамики (CFD). Для численного моделирования использовалась модель k-ε турбулентности. Формула Сазерленда использовалась для определения вязкости воздуха как модели идеального газа.

Результаты: Результаты численного моделирования показывают поведение сверхзвукового обтекания патрона с отделяющимся поддоном. Путем изменения углов открытия лепестков поддона и изменения скорости патрона было выявлено их влияние на аэродинамическое сопротивление, действующее на поддон и сердечник. Это влияние необходимо учитывать в последующих расчетах процесса отделения сердечника и поддона.

Выводы: Исследование показало, что вычислительная аэродинамика может быть использована для получения аэродинамического сопротивления корпуса и сердечника после выхода пули из ствола пистолета. Результаты моделирования, полученные в данной статье, важны для проектирования бронебойных патронов с отделяющимся поддоном.

Ключевые слова: патроны с отделяющимся поддоном, сердечник, аэродинамические характеристики, Ansys Fluent, CFD, численное моделирование.

Nguyen, Q.T. et al, Numerical investigation on the supersonic flow around a saboted bullet, pp.676-694

Нумеричко испитивање надзвучног струјања око поткалибарног пројектила са одвојивим носачем (саботом)

Кван Туан Нуиен, **аутор за преписку,** *Хаи Мин* Нуиен, *Суан Сон* Буи

Државни технички универзитет „Ле Куи Дон", Факултет специјалног машинства, Ханој, Социјалистичка Република Вијетнам

ОБЛАСТ: машинство, динамика флуида
КАТЕГОРИЈА (ТИП) ЧЛАНКА: оригинални научни рад

Сажетак:

Увод/циљ: У овом раду проучавају се аеродинамичке карактеристике специјалног метка при надзвучној брзини. Модел одабран за студију био је пиштољски метак са одвојивим носачем (саботом).

Методе: Коришћен је метод компјутерски симулиране динамике флуида (CFD), а за нумеричку симулацију к-ε модел турбуленције. За вискозност ваздуха, као модела идеалног гаса, примењена је Сатерландова формула.

Резултати: Резултати нумеричке симулације показују понашање надзвучног струјања око метка са одвојивим саботом. Варирањем углова отварања сегмената носача, као и брзине пројектила, утицало је на њихов аеродинамички отпор који делује на носач као и на пенетратор за коришћење у каснијим прорачунима процеса одвајања језгра/пенетратора од носача.

Закључак: Студија показује да се компјутерска аеродинамика може користити за добијање аеродинамичког отпора на носачу и језгру након што метак напусти цев пиштоља. Резултати симулације важни су за пројектовање противоклопних метака са одвојивим носачем.

Кључне речи: противоклопни метак, пиштољ, аеродинамичке карактеристике, Ansys Fluent, CFD, нумеричка симулација.

Paper received on: 21.01.2024.
Manuscript corrections submitted on: 05.06.2024.
Paper accepted for publishing on: 06.06.2024.